Journal of Bio- and Tribo-Corrosion (2018) 4:73
https://doi.org/10.1007/s40735-018-0192-6

Corrosion Protection Effect of Chitosan on the Performance Characteristics of A6063 Alloy

O. S. I. Fayomi[1,3] · I. G. Akande[2] · A. P. I. Popoola[3]

Received: 19 August 2018 / Revised: 26 September 2018 / Accepted: 2 October 2018 / Published online: 8 October 2018

Abstract
This article outlines the behaviour of water-soluble chitosan as an effective inhibitor on aluminium alloy in 3.65% NaCl at room temperature. The inhibitive ability of water-soluble chitosan was examined using electrochemical potentiodynamic polarization techniques, mass loss measurements and computational studies. The outcome of the experiment reveals that chitosan inhibited aluminium alloy in sodium chloride solution exhibits better corrosion protection than the uninhibited because chitosan nanoparticles minimize the ingression of chloride ion into the active sites of aluminium alloy by forming thin film on its surface. The losses in mass by the inhibited aluminium alloy were found to reduce as the concentration of chitosan increases. Results obtained showed that chitosan could offer inhibition efficiency above 70%. Polarization curve demonstrated that chitosan in 3.65% NaCl at room temperature acted as a mixed-type inhibitor. Adsorption of chitosan nanoparticles on the aluminium alloy was found to follow Langmuir adsorption isotherm with correlation regression coefficient (R^2) value of 0.9961.

Keywords Chitosan · Aluminium · Inhibition · Polarization · Langmuir and adsorption

1 Introduction

Aluminium is a metal with many important applications. It is second to iron in terms of production and consumption [1]. As a result of its relevance, the studies of its corrosion behaviour have been attracting considerable attention in various aggressive environments [2–5]. However, aluminium and its alloy exhibit relatively good corrosion resistance compared to iron upon exposure to the atmosphere, which was attributed to a thin oxide film that forms on them [5–7]. However, numerous studies related to the electrochemical behaviour of aluminium and its alloy in sodium chloride solution reveal that they are prone to localized corrosion on exposure to chloride ion [8–12]. Hence, effective corrosion protection measures should be applied. One of these efficient measures is the use of inhibitors. A lot of researches have been carried out to present inhibitors fit for different corrosive media of aluminium and its alloy [13–19].

Researches have also shown that some of inhibitors such as chromates have undesirable effect on the environment [20]. Therefore, it is imperative to study the composition of an inhibitor before usage. However, a large number of inorganic inhibitors have been found to possess good inhibitive performance with low toxicity, but most of them are expensive compared to the organic corrosion inhibitors. Organic corrosion inhibitors, especially those from natural source like chitosan, have become of practical interest nowadays because of their eco-friendly nature. Metal protection by these organic inhibitors comes from the fact that they adsorb on the metal surface forming protective layers against corrosive species in the media [21]. Organic inhibitors effectiveness in corrosion mitigation is a function of several factors such as the nature of the metal surface, the type of corrosive media and the chemical structure of the inhibitor [22, 23]. These factors make it essential for careful choice of inhibitors for metals.

✉ O. S. I. Fayomi
ojosundayfayomi3@gmail.com

✉ I. G. Akande
aigodwin2015@gmail.com

[1] Department of Mechanical Engineering, Covenant University, Ota, Ogun, Nigeria

[2] Department of Mechanical Engineering, University of Ibadan, Ibadan, Oyo, Nigeria

[3] Department of Chemical, Metallurgical and Materials Engineering, Tshwane University of Technology, Pretoria, South Africa

Chitosan's corrosion protection ability is a function of its molecular structure. Naturally, chitosan has electron-rich hydroxyl and amino groups as shown in Fig. 1. These hydroxyl and amino groups have the ability to form bonding on the surface of metals [24, 25] resulting in corrosion protection through coordinate bonding as these electrons are given out freely to the empty or partially occupied Fe orbitals. The choice of chitosan as an inhibitor is drawn from its eco-friendly and adsorption ability on metals [26, 27]. This research aimed at examining the inhibitive ability of chitosan on the corrosion of aluminium alloy in seawater-simulated environment (3.65% NaCl). The effect of chitosan on corrosion behaviour of the aluminium alloy was observed using electrochemical potentiodynamic polarization techniques, mass loss measurements and computational studies.

2 Experimental Procedures

2.1 Sample Preparation

The aluminium alloy coupons used for these studies are of the dimension of (20 × 20 × 2) mm. The spectrometer chemical composition in wt% is shown in Table 1. These coupons were then polished with emery papers of different grades and rinsed with distilled water. Each specimen's weight was recorded and labelled appropriately. 3.65% NaCl solution was prepared using double distilled water which acted as the seawater (corrosive medium). The mass of the chitosan whose molecular structure is shown in Fig. 1 was varied in 3.65% NaCl solution for every potential dynamic polarization measurement taken. For all the electrochemical measurement and mass loss, the volume of prepared solution was 200 ml.

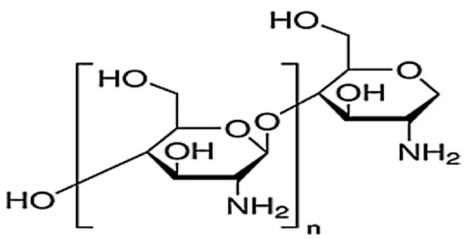

Fig. 1 Molecular structure of chitosan [28]

2.2 Electrochemical Measurement

Autolab PGSTAT 101 Metrohm potentiostat/galvanostat with NOVA software of version 2.1.2 was used for the electrochemical measurements. The aluminium alloy coupon was welded to wire and mounted on resin. Aluminium alloy acted as the working electrode. Graphite rod was used as the counter electrode, and silver chloride electrode (SCE) functions as the reference electrode. Potentiodynamic polarization curves were obtained from potential of −2.0 to −0.5 V versus open circuit potential at a sweep rate (scan rate) of 0.005 V/s.

The working electrode (aluminium alloy) was allowed to immerse in the electrolyte solution (3.65% NaCl) for about 10 min to attain the steady-state potential. The same procedure was carried out with four other aluminium alloy samples varying the concentration of chitosan nanoparticles in four different 200 ml of 3.65% NaCl solution, and the effects were noted. To check for reproducibility, each experiment was repeated four times. The polarization potential (E_{corr}) and current density (I_{corr}) data were evaluated from the Tafel plots. The surface coverage (θ) and the percentage inhibition efficiency ($IE\%$) were calculated from Eqs. (1) to (2) [29–34].

$$\theta = 1 - \frac{i_{corr}}{i_{ocorr}} \tag{1}$$

$$IE\% = 1 - \frac{i_{corr}}{i_{ocorr}} \times 100 \tag{2}$$

where i_{corr} is the inhibited corrosion current densities and i_{ocorr} is the uninhibited corrosion current density.

3 Results and Discussion

3.1 Potentiodynamic Polarization Measurement

Potentiodynamic parameters of aluminium alloy in 3.65% NaCl in the absence and presence of different concentrations of the inhibitor are shown in Table 2, and their corresponding polarization curves are shown in Fig. 2, suggesting that polarization had taken place because of the presence of both cathodic and anodic branches [28, 35].

Evaluation of b_c and b_a (cathodic and anodic slope, respectively), as well as i_{corr} and the corrosion current densities was done by Tafel extrapolation of the current–potential lines at the corresponding values of corrosion potentials (E_{corr}) and is shown in Table 2. The values of corrosion rate (CR) and polarization potential (PR) were also obtained from the Tafel

Table 1 Chemical composition of aluminium alloy (wt%)

Element	S	F	Cu	Mn	Mg	Cr	Ti	Ca	Zr	V	Al
wt%	0.157	0.282	0.0025	0.024	0.51	0.023	0.006	0.0011	0.002	0.0035	Bal.

Table 2 Polarization parameters for inhibited and uninhibited aluminium alloys

Samples	E_{corr} (V)	i_{corr} (μ A/cm^2)	*CR* (mm/year)	b_a (V/dec)	b_c (V/dec)	*PR* (Ω)	*IE* (%)
Control	− 1.308	49.599	0.57634	0.1349	0.15766	236.54	0
Al-0.3CH	− 1.319	19.299	0.22425	0.027876	0.019373	257.21	61.09
Al-0.6CH	− 1.275	18.239	0.21194	0.070823	0.018744	352.91	63.23
Al-0.9CH	− 1.316	14.57	0.13313	0.026102	0.011647	305.29	70.62
Al-1.2CH	− 1.3305	14.16	0.13265	0.12822	0.15991	2707.2	71.45

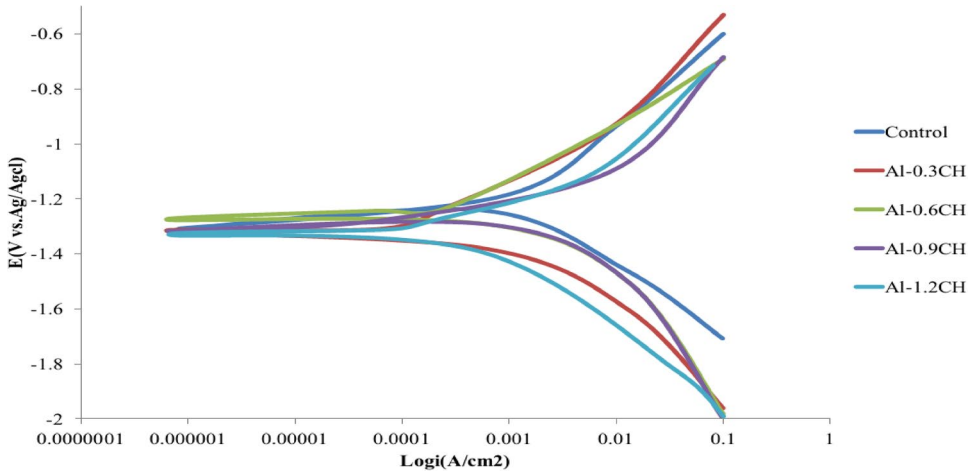

Fig. 2 Potentiodynamic polarization curves for inhibited and uninhibited aluminium alloys

extrapolation. It is worthy of note that the presence of inhibitors causes a decrease in corrosion rate by moving the anodic and cathodic polarization curves in the direction of the lower values of current densities. This prevents the cathodic evolution and anodic metal dissolution reactions of aluminium alloy [36, 37]. The reduction in rate of these reactions increases with an increase in inhibitor concentration. This is an indication that an increase in chitosan nanoparticle from 0.3 g through 0.6 g, 0.9 g and finally 1.2 g drastically hinders the corrosion of aluminium alloy. However, there are little variation in E_{corr} values on varying concentration of Chitosan, suggesting that polarization is a mixed type, which shows that the water-soluble chitosan is a mixed-type inhibitor having adsorbed its molecules on the surface of aluminium alloy [31, 38–41]. But with 1.2 g of chitosan in the salt solution, E_{corr} shifted to a more negative value with respect to others indicating that with higher concentration, chitosan will behave predominantly as cathodic inhibitor in 3.65% NaCl at room temperature.

3.2 Open Circuit Potential (OCP) Measurement

Figure 3 shows the open circuit potential (OCP) versus time curves for aluminium alloy in 3.65% NaCl. Careful examination of the OCP versus time curves reveals that the presences of chitosan shift the steady-state potential towards more negative direction. The negative shift suggests that the cathodic reaction is relatively more affected than the anodic reaction. There were notable changes in the features of the curved compared to the uninhibited sample. The values of OCP for the inhibited samples were between − 0.9 and − 0.92 V within the first 5 s but later moved between more negative value of − 0.92 and − 0.85. It is important to note that the OCP versus time curve for the inhibited and uninhibited aluminium alloy was near straight line, indicating that steady-state potential was attained [42].

3.3 Measurement of Mass Loss and Corrosion Rate

Results obtained from mass loss measurements after the electrochemical experiment using OHAUS pioneer ™PA1214 model are shown in Table 3. Mass loss results indicate that introduction of chitosan into the corrosive medium minimizes corrosion. The loss in mass of aluminium alloy decreases as the concentration of chitosan increases. This is an indication that the mass loss rate had been influenced. Figure 4 shows the effect of chitosan on the corrosion rate of aluminium alloy. The rate of corrosion reduces as the concentration of chitosan increases, which is in accordance with the work of author ref [43]. The corrosion rate of the uninhibited aluminium alloy was found to be the highest on the chart.

3.4 Mechanism of Inhibition Efficiency and Adsorption Study

The values of corrosion current (i_{corr}) in Table 2 and *CR* indicated by Fig. 5 were found to reduce with an increase in

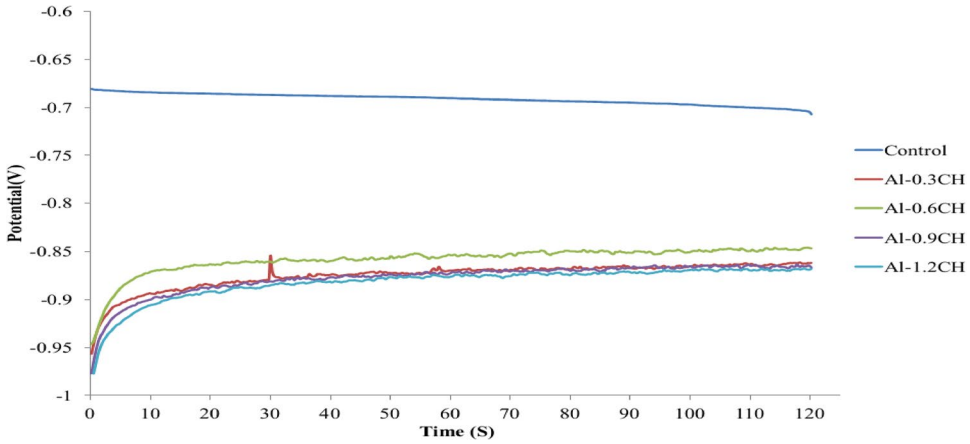

Fig. 3 Evolution of open circuit potential (OCP) versus exposure time for inhibited and uninhibited aluminium alloys in 3.65% NaCl solution

Table 3 Mass loss, surface coverage and C/θ

Samples after immersion	Concentration of chitosan, C (g/l)	Mass loss (mg)	Surface coverage (θ)	C/θ
Control	0	15.4	0	0
Al_1	0.3	7.5	0.611	0.491
Al_2	0.6	6.5	0.632	0.949
Al_3	0.9	6.3	0.706	1.275
Al_4	1.2	4.5	0.715	1.678

the concentration of chitosan, indicating the adsorption of chitosan on the surface of aluminium alloy [44]. The corrosion inhibition efficiency of chitosan increases with an increase in concentration.

In order to have a good knowledge of metal inhibitor interaction and the metallic complex activities on the coverage site, an adsorption mechanism facilitated the computation of C/θ and C for potentiodynamic polarization system using Langmuir adsorption isotherm and a linear relationship [45–47]. Equation (3) shows the Langmuir adsorption isotherm law. The Langmuir isotherm plot in Fig. 6 on the surface features shows a linear relationship with the increase in the concentration of the inhibitor, indicating the continuous adsorption of the inhibitor on the surface of aluminium alloy. The value of (R^2) for Langmuir absorption isotherm was 0.9961. This R^2 value is in the same range as those of Ref. [47, 48]. This showed that the corrosion protection of aluminium alloy by chitosan had been achieved since R^2 is close to unity.

The Langmuir adsorption isotherm law is

$$\frac{C}{\theta} = \frac{1}{K_{\text{ads}}} + C \tag{3}$$

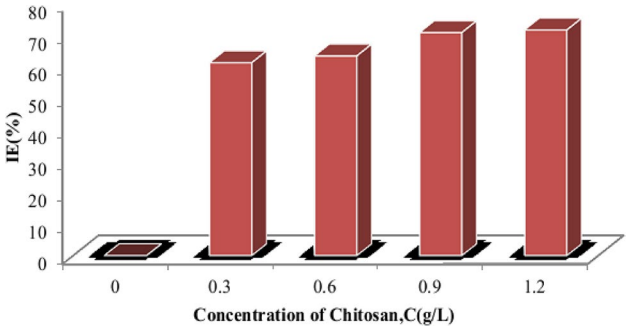

Fig. 5 Variation of inhibition efficiency with an increase in concentration of chitosan

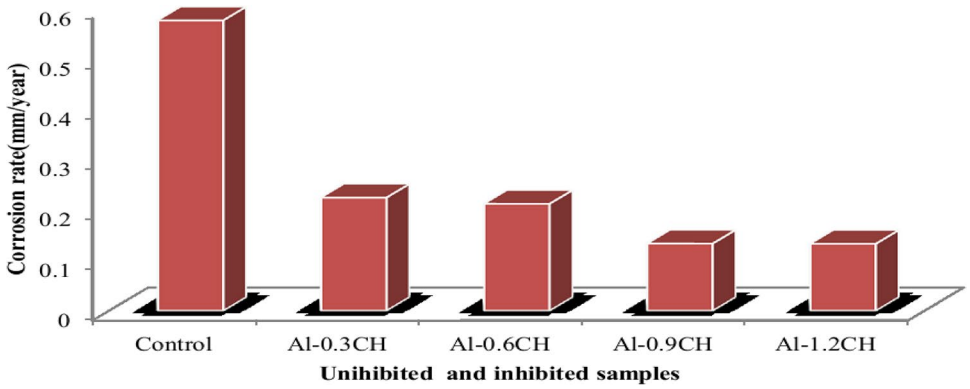

Fig. 4 Representation of rate with respect to the inhibited and uninhibited aluminium alloys

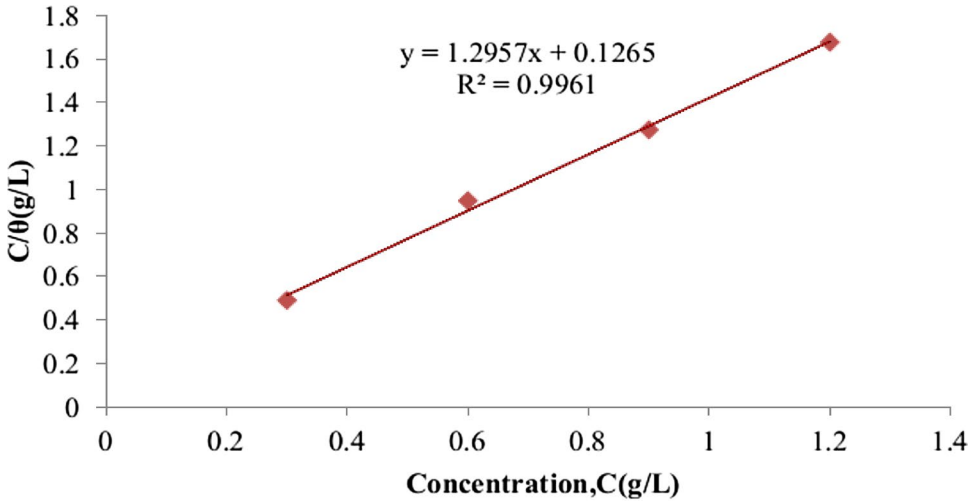

Fig. 6 Langmuir adsorption isotherm for the inhibited samples

where C is the concentration of the corrosion inhibitor, θ is degree of surface coverage, and K is the adsorption equilibrium constant.

4 Conclusions

1. Langmuir adsorption isotherm was obeyed by inhibition of aluminium alloy 3.65% NaCl with correlation regression coefficient of $R^2 = 0.9961$. The values of R^2 are near unity, indicating the effectiveness of the inhibitor
2. Maximum corrosion inhibition efficiency of 71.45% was obtained for the inhibited aluminium alloy in salt solution.
3. The electrochemical potentiodynamic polarization studies show that chitosan acted as a mixed-type inhibitor.
4. Chitosan inhibition efficiency increases with an increase in the inhibitor at room temperature 3.65% NaCl.
5. The corrosion of aluminium alloy substrate in the chloride environment is mitigated by the effective adsorbent of chitosan molecules on aluminium surface. The results of electrochemical techniques and mass loss were in reasonable agreement.

References

1. Prabhu D, Rao P (2013) *Coriandrum sativum* L.: a novel green inhibitor for the corrosion inhibition of aluminium in 1.0 M phosphoric acid solution. J Environ Chem Eng 1(4):676–683
2. Oguzie EE (2007) Corrosion inhibition of aluminium in acidic and alkaline media by *Sansevieria trifasciata* extract. Corros Sci 49(3):1527–1539
3. Li X, Deng S, Fu H (2011) Inhibition by tetradecylpyridinium bromide of the corrosion of aluminium in hydrochloric acid solution. Corros Sci 53(4):1529–1536
4. Oguzie EE, Okolue BN, Ebenso EE, Onuoha GN, Onuchukwu AI (2004) Evaluation of the inhibitory effect of methylene blue dye on the corrosion of aluminium in hydrochloric acid. Mater Chem Phys 87(2–3):394–401
5. Fayomi OS, Abdulwahab M, Popoola AP, Asuke F (2015) Corrosion resistance of AA6063-type Al-Mg-Si alloy by silicon carbide in sodium chloride solution for marine application. J Mar Sci Appl 14(4):459–462
6. Krishnaveni K, Ravichandran J (2014) Effect of aqueous extract of leaves of *Morinda tinctoria* on corrosion inhibition of aluminium surface in HCl medium. Trans Nonferr Metals Soc China 24(8):2704–2712
7. Fayomi OS, Abdulwahab M (2012) Degradation behaviour of aluminium in 2 M HCl/HNO_3 in the presence of *Arachis hypogeae* natural oil. Int J Electrochem Sci 7:5817–5827
8. Halambek J, Berković K, Vorkapić-Furač J (2013) *Laurus nobilis* L.: oil as green corrosion inhibitor for aluminium and AA5754 aluminium alloy in 3% NaCl solution. Mater Chem Phys 137(3):788–795
9. Moore KL, Sykes JM, Hogg SC, Grant PS (2008) Pitting corrosion of spray formed Al–Li–Mg alloys. Corros Sci 50(11):3221–3226
10. Sherif ES (2011) Corrosion and corrosion inhibition of aluminum in Arabian Gulf seawater and sodium chloride solutions by 3-amino-5-mercapto-1,2,4-triazole. Int J Electrochem Sci 6(5):1479–1492
11. Pyun SI, Na KH, Lee WJ, Park JJ (2000) Effects of sulfate and nitrate ion additives on pit growth of pure aluminum in 0.1 M sodium chloride solution. Corrosion 56(10):1015–1021
12. Blücher DB, Svensson JE, Johansson LG (2003) The NaCl-induced atmospheric corrosion of aluminum the influence of carbon dioxide and temperature. J Electrochem Soc 150(3):B93–B98
13. Rahsepar M, Mohebbi F, Hayatdavoudi H (2003) Synthesis and characterization of inhibitor-loaded silica nanospheres for active corrosion protection of carbon steel substrate. J Alloys Compds 709:519–530
14. Umoren SA, Eduok UM (2016) Application of carbohydrate polymers as corrosion inhibitors for metal substrates in different media: a review. Carbohydr Polym 140:314–341
15. Ameh PO, Eddy NO (2014) *Commiphora pedunculata* gum as a green inhibitor for the corrosion of aluminium alloy in 0.1 M HCl. Res Chem Intermed 40(8):2641–2649
16. Akin M, Nalbantoglu S, Cuhadar O, Uzun D, Saki N (2015) *Juglans regia* L.: extract as green inhibitor for stainless steel and aluminium in acidic media. Res Chem Intermed 41(2):899–912

17. Wang Y, Chen Y, Zhao Y, Zhao D, Zhong Y, Qi F, Liu X (2017) A reinforced organic-inorganic layer generated on surface of aluminium alloy by hybrid inhibitors. J Mol Liq 225:510–516
18. Khadraoui A, Khelifa A, Hachama K, Mehdaoui R (2016) *Thymus algeriensis* extract as a new eco-friendly corrosion inhibitor for 2024 aluminium alloy in 1 M HCl medium. J Mol Liq 214:293–297
19. Fayomi OS, Gbenebor OP, Abdulwahab M, Bolu C (2013) Structural modification, strengthening mechanism and electrochemical assessment of the enhanced conditioned AA6063-type Al-Mg-Si alloy. J New Mater Electrochem Syst 16:1–6
20. Winkler DA, Breedon M, White P, Hughes AE, Sapper ED, Cole I (2016) Using high throughput experimental data and in silicon models to discover alternatives to toxic chromate corrosion inhibitors. Corros Sci 106:229–235
21. Umoren SA, Obot IB, Ebenso EE, Okafor PC, Ogbobe O, Oguzie EE (2006) Gum arabic as a potential corrosion inhibitor for aluminium in alkaline medium and its adsorption characteristics. Anti-Corros Methods Mater 53(5):277–282
22. Obot IB, Obi-Egbedi NO, Umoren SA (2009) Antifungal drugs as corrosion inhibitors for aluminium in 0.1 M HCl. Corros Sci 51(8):1868–1875
23. Elgahawi H, Gobara M, Baraka A, Elthalabawy W (2017) Eco-friendly corrosion inhibition of AA2024 in 3.5% NaCl using the extract of *Linum usitatissimum* seeds. J Bio Tribo Corros 3(4):55
24. Menaka R, Subhashini S (2017) Chitosan Schiff base as effective corrosion inhibitor for mild steel in acid medium. Polym Int 66(3):349–358
25. Younes I, Rinaudo M (2015) Chitin and chitosan preparation from marine sources. Structure, properties and applications. Mar Drugs 13(3):1133–1174
26. Jmiai A, El Ibrahimi B, Tara A, Oukhrib R, El Issami S, Jbara O, Bazzi L, Hilali M (2017) Chitosan as an eco-friendly inhibitor for copper corrosion in acidic medium: protocol and characterization. Cellulose 24(9):3843–3867
27. Liu Y, Zou C, Yan X, Xiao R, Wang T, Li M (2015) β-Cyclodextrin modified natural chitosan as a green inhibitor for carbon steel in acid solutions. Indus Eng Chem Res 54(21):5664–5672
28. Solomon MM, Gerengi H, Kaya T, Umoren SA (2017) Enhanced corrosion inhibition effect of chitosan for St37 in 15% H_2SO_4 environment by silver nanoparticles. Int J Biol Macromol 104:638–649
29. Haque J, Verma C, Srivastava V, Quraishi MA, Ebenso EE (2018) Experimental and quantum chemical studies of functionalized tetrahydropyridines as corrosion inhibitors for mild steel in 1 M hydrochloric acid'. Results Phys 9:1481–1493
30. Zakaria K, Negm NA, Khamis EA, Badr EA (2016) Electrochemical and quantum chemical studies on carbon steel corrosion protection in 1 M H_2SO_4 using new eco-friendly Schiff base metal complexes. J Taiwan Inst Chem Eng 61:316–326
31. Dohare P, Chauhan DS, Hammouti B, Quraishi MA (2017) Experimental and DFT investigation on the corrosion inhibition behavior of expired drug lumerax on mild steel in hydrochloric acid anal. Bioanal Electrochem 9:762
32. Anejjar A, El Mouden OI, Batah A, Bouskri A, Rjoub A Corrosion inhibition potential of ascorbic acid on carbon steel in acid media. Appl J Environ Eng Sci 3(1):3–1
33. Yang SF, Wen Y, Yi P, Xiao K, Dong CF (2017) Effects of chitosan inhibitor on the electrochemical corrosion behavior of 2205 duplex stainless steel. Int J Miner Metal Mater 24(11):1260–1266
34. Moses M, Saviour A (2017) Performance evaluation of a chitosan/silver nanoparticles composite on St37 steel corrosion in a 15% HCl solution. ACS Sustain Chem 5(1):809–820
35. Carneiro J, Tedim J, Ferreira MG (2015) Chitosan as a smart coating for corrosion protection of aluminum alloy 2024: a review. Prog Org Coat 89:348–356
36. Dutta A, Saha SK, Adhikari U, Banerjee P, Sukul D (2017) Effect of substitution on corrosion inhibition properties of 2-(substituted phenyl) benzimidazole derivatives on mild steel in 1 M HCl solution: a combined experimental and theoretical approach. Corros Sci 123:256–266
37. Rossrucker L, Samaniego A, Grote JP, Mingers AM, Laska CA, Birbilis N, Frankel GS, Mayrhofer KJ (2015) The pH dependence of magnesium dissolution and hydrogen evolution during anodic polarization. J Electrochem Soc 162(7):333–339
38. Lgaz H, Bhat KS, Salghi R, Jodeh S, Algarra M, Hammouti B, Ali IH, Essamri A (2017) Insights into corrosion inhibition behavior of three chalcone derivatives for mild steel in hydrochloric acid solution. J Mol Liq 238:71–83
39. Perumal S, Muthumanickam S, Elangovan A, Karthik R, Mothilal KK (2017) *Bauhinia tomentosa* leaves extract as green corrosion inhibitor for mild steel in 1 M HCl medium. J Bio Tribo Corros 3(2):13
40. Abd-El-Nabey BA, Goher YM, Fetouh HA, Karam MS (2015) Anticorrosive properties of chitosan for the acid corrosion of aluminium. Port Electrochim Acta 33(4):231–239
41. Fouda AS, Mahmoud WM, Mageed HA (2016) Evaluation of an expired nontoxic amlodipine besylate drug as a corrosion inhibitor for low-carbon steel in hydrochloric acid solutions. J Bio Tribo Corros 2(2):7
42. Gupta RK, Malviya M, Verma C, Quraishi MA (2017) Aminoazobenzene and diaminoazobenzene functionalized graphene oxides as novel class of corrosion inhibitors for mild steel: experimental and DFT studies. Mater Chem Phys 198:360–373
43. Chitra S, Anand B (2017) Surface morphological and FTIR spectroscopic information on the corrosion inhibition of drugs on mild steel in chloride environment. J Chem Pharm Sci 10:453–456
44. Niouri W, Zerga B, Sfaira M, Taleb M, Touhami ME, Hammouti B, Mcharfi M, Al-Deyab SS, Benzeid H, Essassi EM (2014) Electrochemical and chemical studies of some benzodiazepine molecules as corrosion inhibitors for mild steel in 1 M HCl. Int J Electrochem Sci 9:8283–8298
45. Fayomi OS, Abdulwahab M, Durodola BM, Joshua TO, Alao AO, Joseph OO, Inegbenebor AO (2013) Study of the electrochemical behavior and surface interaction of AA6063 type Al-Mg-Si alloy by sodium molybdate in simulated sea water environment. Int J Manage Inform Technol Eng 1(3):159–166
46. Fayomi OS (2014) The inhibitory effect and adsorption mechanism of roasted *Elaeis guineensis* as green inhibitor on the corrosion process of extruded AA6063 Al-Mg-Si alloy in simulated solution. Silicon 6(2):137–143
47. Verma C, Chauhan DS, Quraishi MA (2017) Drugs as environmentally benign corrosion inhibitors for ferrous and nonferrous materials in acid environment: an overview. J Mater Environ Sci 8(11):4040–4051
48. Hameed RA, Al-Shafey HI, Abu-Nawwas AH (2014) 2-(2,6-Dichloranilino)phenyl acetic acid drugs as eco-friendly corrosion inhibitors for mild steel in 1 M HCl. Int J Electrochem Sci 9:6006–6019